MIT Open Access Articles

Hydrogen-Vacancy Interactions in Fe-C Alloys

Massachusetts Institute of Technology

Hydrogen-Vacancy Interactions in Fe-C Alloys

Paul R. Monasterio, Timothy T. Lau, Sidney Yip,[*] and Krystyn J. Van Vliet[†]

*Department of Nuclear Science and Engineering, and Department of Materials Science and Engineering,
Massachusetts Institute of Technology, Cambridge, Massachusetts 02139, USA*

Energetics and concentrations of hydrogen-containing point defect clusters (PDCs) in Fe-C alloys are calculated and cast into a PDC dominance diagram. Because of the strong binding effects of iron vacancies on the stability of the clusters, hydrogen accumulation requires the total hydrogen and vacancy concentrations to be comparable. As a result of the interplay between repulsive and attractive binding processes, PDC populations in Fe-C-H effectively decouple into the binary systems Fe-C and Fe-H. This results in significant vacancy-hydrogen PDC populations even for low total hydrogen concentrations.

In the past few decades, a variety of fundamentally new phenomena has been observed in metals and their alloys under hydrogen-rich conditions, such as large volume contractions in body-centered cubic (bcc) α-Fe [1,2], and the enhancement of diffusion at metal-metal junctions [3]. Furthermore, the well-known problem of hydrogen-induced degradation of the mechanical properties of metals has had significant impact in Fe-rich alloys such as hardened steels that suffer severe embrittlement [4,5]. Experimental and theoretical evidence [1–7] suggests that one unifying theme behind these hydrogen-mediated effects is the strong interaction between hydrogen impurities and other point defects in the material, and the subsequent microstructural changes that occur as a result of that interaction. Although a rich experimental literature detailing macroscopic effects exists, fundamental understanding of the interactions of hydrogen with point defect clusters (PDCs) in metals is limited. In particular, a solid theoretical description of PDC stability, accumulation, and the changes in the PDC concentrations is not yet available.

In this Letter, we study the formation, binding, and concentrations of PDCs in bcc Fe-C alloys containing hydrogen. We use density functional theory (DFT) calculations for the energetics, coupled with a free-energy functional to determine the PDC concentrations as a function of total hydrogen and vacancy concentrations. The processes by which hydrogen binds to PDCs in Fe-C alloys are found to be dominated by the interaction of hydrogen (H) and carbon (C) with bcc iron vacancies (Va). By graphically presenting our results on the PDC concentrations in a dominance diagram, the important role of vacancies in determining the PDC populations is readily appreciated. The PDC dominance representation directly indicates the essential changes in the point defect population as a function of point defect composition in the alloy bulk, analogous in spirit to a phase diagram. An effective decoupling between the Va_xH_z and Va_xC_y populations is found, simplifying the full Fe-C-H system into a superposition of the PDC populations of the Fe-C and Fe-H binary systems. The strong Va-H interaction implies that the accumulation of hydrogen into PDCs comprising molecular hydrogen (H_2) is favored over PDCs containing atomic hydrogen only in a bounded range of total Va concentrations.

The total energy DFT calculations were performed using the VASP code [8] with Blöchl's projector augmented method [9]. Calculations were carried out with a plane-wave energy cutoff of 400 eV in 128-atom supercells with the theoretical lattice constant of 2.835 Å, using a $2 \times 2 \times 2$ k-point mesh for integration over the Brillouin zone and a Methfessel Paxton Fermi-surface smearing parameter of 0.05 eV [10]. Calculations included spin polarization effects and assumed an initial ferromagnetic charge density consistent with the bcc ferritic Fe phase. No symmetry constraints were imposed. The geometric relaxation was terminated with a force cutoff of 5 meV/Å. Vibrational frequency calculations were performed in 54-atom supercells with the same k-point mesh. Results are reported at a benchmark temperature of 160 °C, representative of the tempering temperatures for carbon-rich bcc Fe-C alloys. Numerous shallow local energy minima exist near the optimized geometry for a given PDC stoichiometry, and hence the use of straightforward energy minimization procedures is limited. This results in an error for the binding energies of approximately 0.1 eV, implying an error in the magnitude of the defect cluster concentrations of, at most, 2 orders of magnitude at 160 °C. However, as shown subsequently, conclusions regarding the dominant PDC types as a function of alloy composition are not modified by this level of uncertainty.

Calculations are performed with a constrained grand canonical free-energy functional, similar to what we have presented previously for the bcc Fe-C binary alloy [11], in order to account for the variable concentrations of PDC in the system and obtain a unique solution. Specifically, the formation energy of each PDC in a closed Fe-C-H system is given by

$$E_{\text{form}}^{D}(T, \mu_{\text{Fe}}, \mu_{\text{H}}, \mu_{\text{C}}) = E^{D}(T) - E^{0}(T) - \mu_{\text{Fe}}\Delta n_{\text{Fe}}$$
$$- \mu_{\text{C}}\Delta n_{\text{C}} - \mu_{\text{H}}\Delta n_{\text{H}}, \quad (1)$$

where $E^D(T)$ and $E^0(T)$ are the DFT-calculated free energies (only including vibrational entropy) for the PDC-containing and perfect supercells, respectively, μ_X is the chemical potential of element X, and Δn_X is the difference in the number of atoms of element X in the two cells. Vibrational contributions to the free energy are obtained by approximating the atoms as 3D harmonic oscillators with DFT-calculated frequencies. The binding energy for point defect cluster D comprising n_{Va} vacancies, n_{C} carbon atoms, and n_{H} hydrogen atoms relative to the elementary defects (free vacancies, octahedral carbon, and tetrahedral hydrogen interstitials) is computed by

$$E_{\text{binding}}(T) = n_{\text{Va}}E^{\text{Va}}_{\text{form}}(T) + n_{\text{C}}E^{\text{C}}_{\text{form}}(T) + n_{\text{H}}E^{\text{H}}_{\text{form}}(T),$$
(2)

where $E^D_{\text{form}}(T)$ is defined in (1), and here normalized by corresponding chemical potentials, and $E^{\text{Va}}_{\text{form}}(T)$, $E^{\text{C}}_{\text{form}}(T)$, and $E^{\text{H}}_{\text{form}}(T)$ are the formation energies for free vacancies, octahedral carbon, and tetrahedral hydrogen interstitials, respectively. Binding energies at 0 K and 433 K (160 °C) for dominant PDCs (15 out of 38 PDCs studied) are summarized in Table I. At 0 K, the formation energy for a C octahedral is 0.86 eV lower than that for a C tetrahedral interstitial, consistent with experimental observations [12]. In contrast, hydrogen is more stable in a tetrahedral site, with a calculated formation energy 0.12 eV lower than that for an octahedral hydrogen site, also consistent with empirical data [14].

Equilibrium PDC concentrations are calculated by minimizing the Helmholtz free energy of the system

TABLE I. Selected binding free energies for different defect stoichiometries at 0 K and 433 K (160 °C). Only the deepest energy minimum for each defect PDC stoichiometry is shown. Experimental values are given in parentheses for comparison, where available.

PDC	E_{binding} (eV)	
	$T = 0$ K	$T = 433$ K
$H_{\text{octahedral}}$	−0.12 (−0.07 [12])	−0.18
$C_{\text{tetrahedral}}$	−0.86	−0.84
Va_1H_1	0.51 (0.46 [13])	0.61
$Va_2H_1\langle 100 \rangle$	0.76	1.05
$Va_2C_1\langle 100 \rangle$	1.04	1.20
C_1H_1	0.02 (0.03 [13])	0.02
$Va_1C_1H_1$	1.14	1.31
$Va_1C_2H_1$	1.38	1.63
$Va_2C_1H_1\langle 111 \rangle$	0.86	1.20
$2H = H_2$	0.01 (0.04 [13])	0.004
Va_1H_2	0.98	1.18
$Va_2H_2\langle 100 \rangle$	1.22	1.65
C_1H_2	−0.05	0.01
$Va_1C_1H_2$	0.92	1.19
Va_1H_3	1.38	0.82

$$F(T, \mu_{\text{Fe}}, \mu_{\text{H}}, \mu_{\text{C}}) = \sum_i n_i E_{\text{form}}(T, \mu_{\text{Fe}}, \mu_{\text{H}}, \mu_{\text{C}})$$
$$- k_B T \sum_i \ln\left(\frac{(\alpha_i N)!}{(\alpha_i N - n_i)! n_i!}\right),$$
(3)

where the first term is described in (1) and the second term accounts for the configurational entropy of the system; k_B represents Boltzmann's constant and T the absolute temperature. Here, n_i is the total number of PDCs of type i, N is the total number of bcc lattice positions, and α_i is defined such that $\alpha_i N$ is the number of indistinguishable configurations in the lattice for the defect cluster i for large N. For example, for free vacancies $\alpha_i = 1$, because any bcc lattice site could serve as a possible Va site, while for a tetrahedral interstitial $\alpha_i = 6$ because there are six tetrahedral sites for each bcc lattice site. The entropic term in (3) counts the number of possible ways to rearrange the PDC in the crystalline lattice. Minimizing the free energy in (3) and defining the defect concentration of a given PDC with respect to the bcc Fe lattice by $c_i = \frac{n_i}{N}$ we find

$$c_i = \frac{\alpha_i}{\exp\left(\frac{E_{\text{form}}(T, \mu_{\text{Fe}}, \mu_{\text{H}}, \mu_{\text{C}})}{k_B T}\right) + 1}.$$
(4)

The chemical potentials are related to the total concentrations of C, H, and Va by the following constraints:

$$\text{Va}_{\text{tot}} = \sum_{\text{clusters}} x[\text{Va}_x\text{C}_y\text{H}_z]$$
(5)

$$\text{C}_{\text{tot}} = \sum_{\text{clusters}} y[\text{Va}_x\text{C}_y\text{H}_z]$$
(6)

$$\text{H}_{\text{tot}} = \sum_{\text{clusters}} z[\text{Va}_x\text{C}_y\text{H}_z],$$
(7)

where $[\text{Va}_x\text{C}_y\text{H}_z]$ is the concentration of a particular PDC type calculated from (4) that comprises x iron vacancies, y carbon atoms, and z hydrogen atoms. Figure 1 shows these results in a PDC dominance diagram. Boundaries are determined by changes in the most dominant PDC, dividing the diagram into nine distinct regions, each characterized by a single prevalent PDC. Statistically relevant, but non-dominant PDCs (defined in this study as PDCs with concentrations within 2 orders of magnitude of the most prevalent one), vary in concentration within a given zone and thus their precise concentration ranking is not reported. Figure 1 thus indicates which PDCs are of macroscopic importance for a given alloy composition and point defect concentration, providing a framework to delve into more detailed analysis of the microstructure. A full dominance representation ordinarily would require a three dimensional graph indicating the prevalent PDCs as a function of total C, H, and Va concentrations. However, since our interest lies primarily on the effects of hydrogen, we focus on the changes as a function of the $[H_{\text{tot}}]$ and $[Va_{\text{tot}}]$. Thus, although our methodology can generate the full diagram,
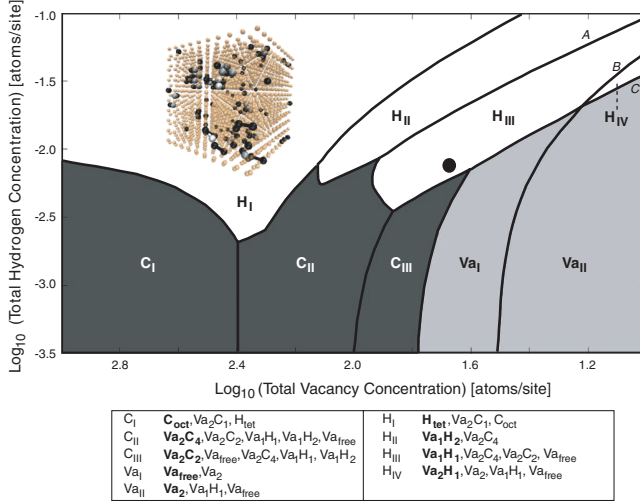
FIG. 1 (color online). Dominance diagram for PDCs in Fe-C-H alloys with $[C_{tot}] = 0.01$ (1.0 at. %). The PDC of highest concentration in each zone is indicated in bold, and other statistically relevant PDCs are listed. The A, B, and C boundaries in the high $[H_{tot}]$, high $[Va_{tot}]$ regime are also indicated. The inset shows a schematic of the defect population at the marked point. Vacancies (black), hydrogen (white), and carbon (gray) atoms bind in a background bcc Fe matrix (orange). Va_2 clusters are oriented along the $\langle 111 \rangle$ direction.

the total carbon concentration is fixed to be that reported for high-carbon steels ($[C_{tot}] = 0.01$ in Fig. 1) [11].

Most zones in the diagram, except for H_I and C_I, are dominated by Va-containing PDCs. Thus, the vacancy-mediated interactions are the primary factors that determine the PDC populations in the alloy, and the full complexity of the PDC spectrum can only be appreciated in the regime in which $[Va_{tot}]$ is significant. In the C and H regions of the diagram, these Va-containing PDCs exhibit concentrations many orders of magnitude higher than the free vacancies and divacancy clusters. Hence, consistent with previous studies [15], the presence of hydrogen is observed to stabilize free vacancies in bcc Fe, in the form of vacancy-solute clusters. In addition, for $[H_{tot}] \gg [C_{tot}]$, and low $[Va_{tot}]$ (H_I zone), interstitial atomic hydrogen is prevalent over molecular hydrogen ($E_b = 0.004$ eV), in the constrained geometries of the bcc Fe lattice, and hydrogen accumulation is not thermodynamically favored. Nonetheless, once one or multiple vacancies are present, the formation energy for molecular hydrogen (H_2) is substantially lowered and the formation of localized clusters containing multiple hydrogen atoms is facilitated (H_{II} zone). On the other hand, the stabilizing effect of H in Va-only PDCs implies that the most significant defect clusters in the alloy contain H_2 only up to a maximum $[Va_{tot}]$, which, in principle, is amenable to experimental comparison. This maximum is denoted by boundary A between the H_{II} and H_{III} zones, and is approximately linear on $[H_{tot}]$, i.e., $(2\frac{[H_{tot}]}{3})^{0.9}$. Above this upper bound, atomic

hydrogen-containing PDCs again dominate (as in H_I). In this regime ($[H_{tot}] \gg [C_{tot}]$), as vacancy concentrations increase for a fixed $[H_{tot}]$, dominant PDCs first switch from tetrahedral hydrogen interstitials to Va_1H_2 (zone H_{II}); upon crossing zone boundaries A, B, and C, stoichiometry of the dominant PDC then changes from Va_1H_1 (zone H_{III}) to Va_2H_1 (zone H_{IV}) to Va-only PDCs (zone Va_{II}), respectively.

Turning now to regions in which all three point defect types (Fe vacancies, H, and C) interact and carbon-containing PDCs are statistically relevant, the full complexity of the PDC populations is apparent. Interactions between hydrogen and carbon interstitials are similarly mediated by vacancies. Our energy calculations (Table II) show which binding mechanisms are thermodynamically disfavored for H and C in the presence of Va. We observe that hydrogen does not bind with carbon in the absence of iron vacancies. This is consistent with observations showing that hydrogen is repelled from regions of high mass and charge density [6] such as interstitial carbon atoms within the highly confined geometry of the bcc Fe lattice. Furthermore, as shown in the second reaction in Table II, hydrogen is unable to displace carbon from existing PDCs and instead binds to those clusters. The absorption of hydrogen into larger PDCs is also thermodynamically favored (Table III). However, as the number of solute atoms in the PDC grows, the presence of additional vacancies is required to promote hydrogen binding. Alternatively, appreciable lattice distortions in the form of extended defects, such as precipitate interfaces [4], can provide an analogous effect to that of vacancies in the bulk lattice by facilitating C-H binding. The combination of the two competing processes of hydrogen-carbon interactions (repulsion in the absence of vacancies but high affinity when mediated by vacancies) results in an effective decoupling of the Va_xH_z and Va_xC_y PDC populations; that is, vacancy-solute (Va-H and Va-C) interactions become the primary contributors to the binding processes. The remaining interactions which complete the three-body description of this alloy, i.e., the C-H and Va-C-H interactions, represent a substantially less significant effect in terms of determining the type and concentration of PDCs. In particular, for low total vacancy concentrations, no dominance zone in which C_yH_z PDCs dominate exists. Furthermore, as can be seen in Fig. 1, in the regime in which $[H_{tot}] \sim 0.1[C_{tot}]$, the spectrum of the Fe-C-H system shows a rich variety of statistically relevant PDC types due to the vacancy-mediated interactions. Therefore, the

TABLE II. Energy changes in binding reactions involving the Va_1C_1 and H_{tet} PDCs.

Reaction	$\Delta E_{reaction}$ (eV)
$Va_1C_1 + H_{tet} \rightarrow Va_1C_1H_1$	-0.62
$Va_1C_1 + H_{tet} \rightarrow Va_1H_1 + C_{oct}$	0.01

TABLE III.   Energy changes in binding reactions involving the Va_1C_2 and $Va_2C_1\langle 100\rangle$ PDCs.

Reaction	$\Delta E_{reaction}$ (eV)
$Va_1C_2 + H_{tet} \rightarrow Va_1C_2H_1$	0.06
$Va_1C_2 + H_{tet} \rightarrow Va_1C_1H_1 + C_{oct}$	0.30
$Va_2C_1 + H_{tet} \rightarrow Va_2C_1H_1$	-0.33
$Va_2C_1 + H_{tet} \rightarrow Va_2H_1 + C_{oct}$	14.6

dominance of specific PDCs in this regime is strongly dependent on $[Va_{tot}]$ in a highly nontrivial manner. Nonetheless, the transition from atomic to molecular to atomic hydrogen is preserved as $[Va_{tot}]$ increases, though these PDCs are no longer dominant.

For low $[Va_{tot}]$ (in this regime in which $[H_{tot}] \sim 0.1[C_{tot}]$), carbon interstitials are the prevalent PDC (C_I zone) and no binding between H and C is found to occur. Clusters containing both H and C, such as $Va_1C_1H_1$ or $Va_2C_2H_1$ PDCs, are never statistically relevant. As $[Va_{tot}]$ increases, Va_2C_4 clusters become the dominant PDC (C_{II} zone), and the concentration of hydrogen-containing PDCs such as Va_1H_1 and Va_1H_2 also increases. In fact, the addition of H pushes the system into the high-hydrogen regime of the C_{II} zone, rendering the Va_1H_1 and Va_2H_1 PDCs statistically relevant. Based on experimental observations of rapid hydrogen diffusion [3] and given the relatively small radius of the hydrogen atom as compared to bcc Fe vacancies and interstitials, we conjecture that these small Va_xH_z PDCs should be highly mobile, therefore having important macroscopic consequences which can be tested experimentally. Direct calculation of these PDC migration mechanisms and lowest energy barriers will be a topic of future studies. When the total hydrogen and carbon concentrations become more similar (e.g., $[H_{tot}] = [C_{tot}] = 0.01$), the relative dominance in the diagram changes. Carbon-free defect clusters such as Va_1H_1 (lower end of the H_{III} zone) and Va_1H_2 (lower end of the H_{II} zone) become the dominant PDC. However, Va_2C_4 and Va_2C_2 PDCs remain of significant concentration throughout the $[Va_{tot}]$ range examined. Although never significant, $Va_2C_2H_1$ clusters (divacancies oriented in the $\langle 111\rangle$ direction of the bcc Fe lattice) approach significant concentrations when $[Va_{tot}]$ becomes comparable to $[C_{tot}]$ and $[H_{tot}]$; however, in this range, the concentration of several Va_xC_y and Va_xH_z clusters also increases such that the $Va_2C_2H_1$ clusters represent only a minor fraction of the overall PDC spectrum. Similarly, $Va_1H_1C_1$ PDCs are never present in significant proportions, underscoring the effective decoupling of the Fe-C and Fe-H PDC populations.

This decoupling of the PDC types provides a simplifying framework for the study of hydrogen binding in alloys of more complex composition and/or crystalline defect types. Moreover, these observations inform macroscopic con-

cerns of hydrogen damage by indicating conditions under which mechanisms of primary degradation by internal hydrogen pressure buildup [4] (i.e., H accumulation) are viable. For such processes to occur, the local vacancy concentration must be such that molecular hydrogen formation is favored, such as in the neighborhood of a microvoid or microcrack [4]. In other words, the point defect composition must be within the H_{II} dominance zone in Fig. 1. Finally, given the high concentration of Va_1H_1 and Va_1H_2 PDCs, even when total hydrogen concentrations are relatively small ($[H_{tot}] < 10^{-2.5}$ or 0.3 at. % at the top of C_{II} and C_{III}), these PDCs are likely to be responsible for macroscopic effects which are controlled by the diffusion of Va (and Va-containing PDCs) towards line and surface defects such as dislocations or grain boundaries. The results presented herein, which predict PDC populations in the lattice of the bulk alloy, could be the basis for studies of point- and such extended-defect interactions, the importance of local PDCs in the neighborhood of such defects and the differences from bulk properties, and the associated macroscopic consequences of hydrogen-induced phenomena.

*syip@mit.edu
†krystyn@mit.edu

[1] Y. Fukai and N. Okuma, Jpn. J. Appl. Phys. **32**, L1256 (1993).
[2] M. Iwamoto and Y. Fukai, Mater. Trans., JIM **40**, 606 (1999).
[3] E. Hayashi, Y. Kurokawa, and Y. Fukai, Phys. Rev. Lett. **80**, 5588 (1998).
[4] J. P. Hirth, Metall. Trans. A **11A**, 861 (1980).
[5] M. Nagumo, M. Nakamura, and K. Takai, Metall. Mater. Trans. A **32A**, 339 (2001).
[6] S. M. Myers *et al.*, Rev. Mod. Phys. **64**, 559 (1992).
[7] G. Lu and E. Kaxiras, Phys. Rev. Lett. **94**, 155501 (2005).
[8] G. Kresse and J. Furthmüller, Phys. Rev. B **54**, 11169 (1996).
[9] P. E. Blöchl, Phys. Rev. B **50**, 17953 (1994).
[10] M. Methfessel and A. T. Paxton, Phys. Rev. B **40**, 3616 (1989).
[11] C. Först, J. Slycke, K. Van Vliet, and S. Yip, Phys. Rev. Lett. **96**, 175501 (2006).
[12] A. Vehanen *et al.*, Phys. Rev. B **25**, 762 (1982).
[13] C. G. Chen and H. K. Birnbaum, Phys. Status Solidi A **36**, 687 (1976).
[14] H. D. Carstanjen, Phys. Status Solidi A **59**, 11 (1980).
[15] Y. Tateyama and T. Ohno., Phys. Rev. B **67**, 174105 (2003).